Estimating Daily Net Radiation over Vegetation Canopy through Remote Sensing and Climatic Data

Zohrab Samani[1]; A. Salim Bawazir[2]; Max Bleiweiss[3]; Rhonda Skaggs[4]; and Vien D. Tran[5]

Abstract: Net radiation (R_n)=key variable in hydrological studies. Measured net radiation data are rarely available and are often subject to error due to equipment calibration or failure. In addition, point measurements of net radiation do not represent the diversity of the regional net radiation values which are needed for large scale evapotranspiration mapping. A procedure has been developed to estimate daily net radiation using canopy temperature, albedo, short wave radiation and air temperature. This procedure makes it possible to estimate R_n by combining information from satellite and local weather stations. Three different methodologies are presented to estimate net radiation. Comparisons between net radiation using the three methods resulted in average error ranging from 1 to 30% and standard error of estimate ranging from 1.06 to 5.34 MJ/m^2/day.

DOI: 10.1061/(ASCE)0733-9437(2007)133:4(291)

CE Database subject headings: Evapotranspiration; Net radiation; Satellite; Solar radiation; Weather station; Classification description; Irrigation and drainage.

Introduction

Net radiation (R_n)=key parameter in computing reference evapotranspiration and is a driving force in many other physical and biological processes (Rosenberg et al. 1983). However, direct measurement of R_n continues to be a challenge for researchers. In many physical, agronomical and biological applications, R_n rather than solar radiation (R_s) is required. Despite the many applications for R_n, the net radiation data are rarely available due to the technical and economical limitations associated with direct measurements. Even when the net radiation is available it is usually limited to a small area and does not represent the spatial variability. For example, the ASCE standardized reference evapotranspiration equation (Allen et al., 2005) has recommended a method to estimate daily net radiation from solar radiation, albedo, humidity and air temperatures. However, this methodology is limited to estimating R_n over a well-watered grass canopy and can not be used to estimate R_n over other vegetations and areas with sparse and/or stressed vegetation conditions.

Samani et al. (2005) presented a methodology to estimate daily net radiation over plant canopy by using canopy temperature, albedo and R_s. The methodology was based on a procedure initially developed by Bastiaanssen (1995) for estimating incident net radiation (R_{ni}). Bastiaanssen (1995) proposed the following equation to estimate R_{ni} as

$$R_{\mathrm{ni}} = (1-\alpha)R_{\mathrm{si}} + \mathrm{RL}{\downarrow} - \mathrm{RL}{\uparrow} - (1-\varepsilon_0)RL{\downarrow} \qquad (1)$$

where R_{ni}=incident (instantaneous) net radiation (W/m^2); R_{si}=incident incoming short wave radiation (W/m^2); RL↓=incident incoming longwave radiation (W/m^2); RL↑=incident outgoing longwave radiation (W/m^2) α=surface albedo (dimensionless); and ε_0=surface emissivity (dimensionless).

R_{si} for clear sky can be calculated using the following equation:

$$R_{\mathrm{si}} = G_{\mathrm{sc}} \cos\theta d_r \tau_{sw} \qquad (2)$$

where; G_{sc}=solar constant (1,367 W/m^2) θ=solar incidence angle; and d_r=inverse relative earth–sun distance (Allen et al. 1998) is calculated as

$$d_r = 1 + 0.033\cos\left(\frac{2\pi}{365}J\right) \qquad (3)$$

where J=Julian day of the year. τ_{sw}=atmospheric transmissivity from elevation (Allen et al. 1998), calculated as

$$\tau_{sw} = 0.75 + 2\times10^{-5}(Z) \qquad (4)$$

where Z=elevation (m). RL↓ and RL↑ are calculated as follows:

$$\mathrm{RL}{\downarrow} = \varepsilon_a \sigma T_i^4 \qquad (5)$$

where ε_a=atmospheric emissivity calculated using the following equation (Bastiaanssen 1995):

$$\varepsilon_a = 0.85(-\ln\tau_{sw})^{0.09} \qquad (6)$$

where σ=Stefan–Boltzman constant (5.67×10^{-8} W/m^2/K^4); T_i=incident near surface air temperature, K; and

[1]Professor, New Mexico State Univ., MSC 3CE, Las Cruces, NM 88003.

[2]Assistant Professor, New Mexico State Univ., MSC 3CE, Las Cruces, NM 88003.

[3]Research Specialist, New Mexico State Univ., MSC 3CE, Las Cruces, NM 88003.

[4]Professor, New Mexico State Univ., MSC 3169, Las Cruces, NM 88003.

[5]Graduate Student, New Mexico State Univ., MSC 3CE, Las Cruces, NM 88003.

Note. Discussion open until January 1, 2008. Separate discussions must be submitted for individual papers. To extend the closing date by one month, a written request must be filed with the ASCE Managing Editor. The manuscript for this paper was submitted for review and possible publication on January 13, 2006; approved on January 30, 2007. This paper is part of the ***Journal of Irrigation and Drainage Engineering***, Vol. 133, No. 4, August 1, 2007. ©ASCE, ISSN 0733-9437/2007/4-291–297/$25.00.

$$\mathrm{RL}\uparrow = \varepsilon_0 \sigma T_s^4 \tag{7}$$

where ε_o=surface emissivity (dimensionless), calculated as ε_0=0.95+0.01 LAI when LAI<3 and ε_0=0.98 when LAI⩾3 LAI=leaf; area index; and T_s=incident surface temperature (K).

Surface temperature can be measured from satellite or ground sensors. Solar incident angle, θ, in Eq. (2), can be calculated from the following equation (Tasumi et al. 2000, Recktenwald 2004):

$$\begin{aligned}\cos(\theta) = {} & \sin(\delta)\sin(\phi)\cos(\beta) - \sin(\delta)\cos(\phi)\sin(\beta)\cos(\gamma) \\ & + \cos(\delta)\cos(\phi)\cos(\beta)\cos(\omega) \\ & + \cos(\delta)\sin(\phi)\sin(\beta)\cos(\gamma)\cos(\omega) \\ & + \cos(\delta)\sin(\beta)\sin(\gamma)\sin(\omega)\end{aligned} \tag{8}$$

where; δ=solar declination (rad), which is calculated from the following equation (Allen et al. 1998):

$$\delta = 0.409 \sin\left(\frac{2\pi}{365}J - 1.39\right) \tag{9}$$

ϕ=latitude of the site; β=downward slope, where β=0 for horizontal surface and β=π/2 for vertical surface, β is always positive and represents downward slope in any direction; γ=deviation of the normal to the surface from the local meridian; and ω=solar time angle (rad), and is calculated from the following equation:

$$\omega = \frac{\pi}{12}(\mathrm{LST} - 12) \tag{10}$$

where LST=local solar time (h), which is defined by the location of the sun in the sky. At solar noon, LST=12:00, and the sun is at its highest point in the sky. Local solar time is calculated from the following equation:

$$\mathrm{LST} = t + 0.06667(L_{\mathrm{std}} - L_{\mathrm{loc}}) + S_c - \mathrm{DT} \tag{11}$$

where T=local civil time (Pacific Standard Time, Eastern Standard Time, etc.); L_{std}=longitude (deg) of the standard meridian in the local time zone (degrees west of Greenwich), for example, L_{std}=75, 90, 105, and 120° for Eastern, Central, Rocky Mountain, and Pacific time zones in the United States, respectively; L_{loc}=local longitude (deg) west of Greenwich; DT=1 if daylight saving time is in effect, DT=0 otherwise; and S_c=correction (h), which accounts for perturbation in earth's rotation rate and is calculated as

$$S_c = 0.1645 \sin(2b) - 0.1255 \cos(b) - 0.025 \sin(b) \tag{12}$$

and

$$b = \frac{2\pi(J - 81)}{364} \tag{13}$$

If short wave solar radiation data are available, then they should be used directly in Eq. (1) to calculate R_{ni}. Values of albedo, surface temperature, and LAI can be measured at the site or obtained from periodic satellite data. Assuming that the positive net radiation received during the daytime (referred to as daily net radiation) is proportional to the short wave solar radiation, Samani et al. (2005) proposed the following equation to estimate daily R_n from R_{ni} and values of short wave radiations (R_s and R_{si}).

$$\frac{R_{\mathrm{ni}}}{R_n} = \frac{R_{\mathrm{si}}}{R_s} \tag{14}$$

Rearranging Eq. (14), the daily net radiation can be calculated as

$$R_n = R_{\mathrm{ni}}\left(\frac{R_s}{R_{\mathrm{si}}}\right) \tag{15}$$

To prove the concept, measured values of daily net radiation (R_n) were compared with predicted values of R_n using measured daily R_s and measured incident net (R_{ni}) and short wave (R_{si}) radiation values. The incident radiation values used in the calculations were measured at 11:00 a.m Mountain Standard Times. Short wave solar radiation was measured at Chamberino Weather Station, New Mexico (latitude 32.06N, longitude 106.68W, elevation 1,145 m) using a LI-COR silicon pyranometer (Model LI200X-L, Campbell Scientific Inc, Logan, Utah) and the net radiation was measured using a net radiometer Model No. Q7.1 (Radiation and Energy Balance Systems, Inc., Seattle) installed about 2.5 m above the vegetation canopy. The same measurements were also available for two riparian vegetations in the Middle Rio Grande flood plain at Bosque del Apache National Wildlife Refuge referred to herein as the Bosque, located about 21 km south of Socorro in central New Mexico with average elevation of 1,370 m.

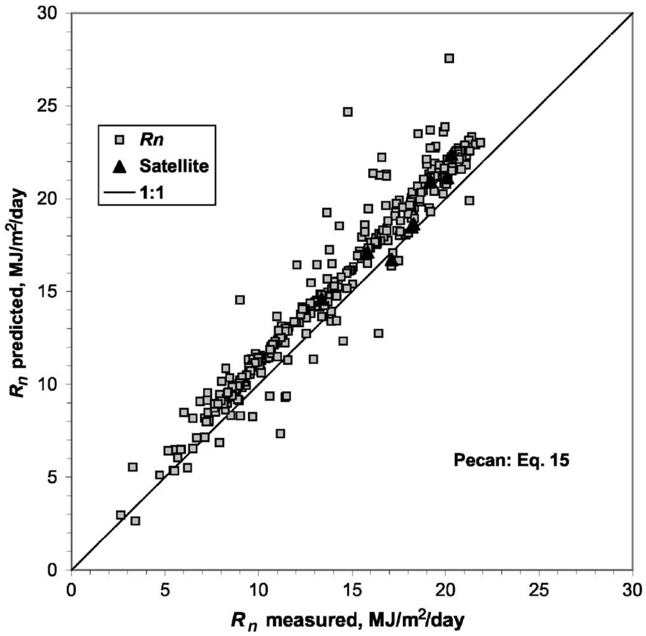

Fig. 1. Predicted and measured net radiation over pecan canopy using Eq. (15)

Fig. 1 compares measured and predicted values of daily net radiation over a pecan canopy located about 13 km south of Las Cruces, N.M. (latitude 32.18N longitude 106.74 W, elevation 1,144 m). The data presented here were measured in 2003. The results showed that Eq. (15) tended to overestimate the daily net radiation values in most cases. This overestimation is the result of disparity between incident temperature and average daily temperature. The higher value of air temperature at 11:00 a.m. (Mountain Standard Time) resulted in overestimation of incoming incident long wave radiation thus resulting in overestimation of incident and daily net radiation. Consequently, a modified form of Eq. (15) was introduced to account for the effect of incident air temperature on R_n prediction. The modified equation is

$$R_n = R_{\mathrm{ni}}\left(\frac{R_s}{R_{\mathrm{si}}}\right)\left(\frac{T_a}{T_i}\right)^4 \tag{16}$$

where T_i=incident air temperature and T_a=average of daily maximum and minimum air temperatures (K).

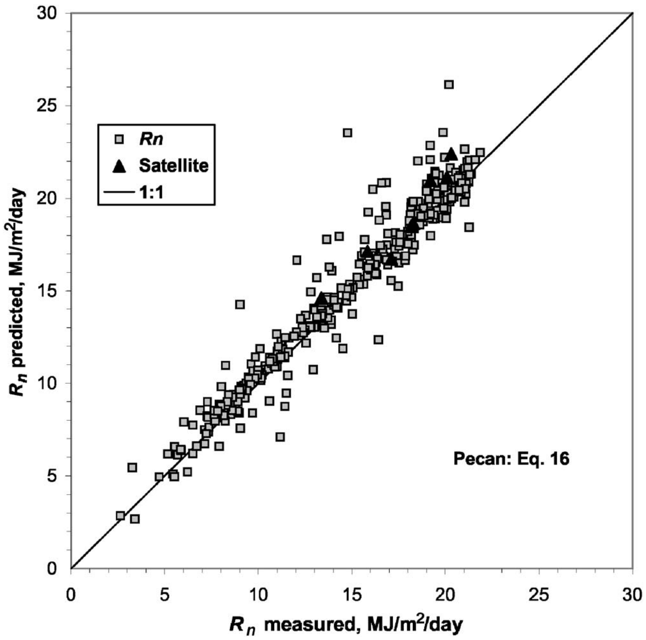

Fig. 2. Predicted and measured net radiation over pecan canopy using Eq. (16)

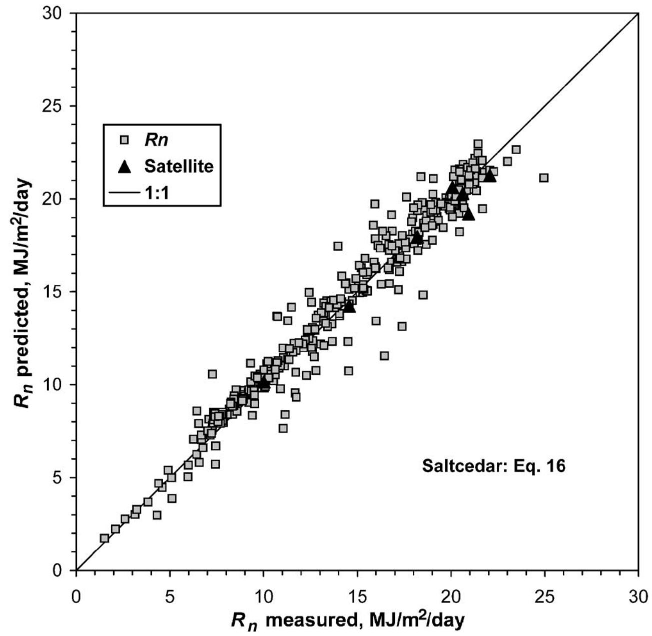

Fig. 3. Comparison between measured and estimated R_n values in saltcedar at Bosque

Eq. (16) accounts for the overestimation of R_n by correcting for the overestimation of incoming incident long wave radiation. This paper presents three different methods to evaluate the accuracy of Eq. (16) in predicting net radiation as follows:

- Method "a" calculates R_n using ground measurement of R_{si}, R_{ni}, R_s, T_i, and T_a;
- Method "b" calculates R_n using satellite measurements of albedo, normalized difference vegetation index (NDVI), surface temperature, air temperature and daily solar radiation (R_s) from weather station; and
- Method "c" calculates R_n using satellite measurements of albedo, NDVI, surface temperature, and estimated values of daily solar radiation (R_s) based on daily maximum and minimum air temperature, (Hargreaves and Samani 1982).

Method a

Fig. 2 compares the predicted and measured R_n for pecan based on Method a. The ratio of predicted over measured values in Fig. 2 was 1.04 and the standard error of estimate (SEE) was 1.65 MJ/m^2/day. The SEE which is the dispersion of the observed values about the regression line or a measure of accuracy of prediction was calculated as follows:

$$\mathrm{SEE} = \sqrt{\frac{\sum (Y - Y')^2}{n-1}} \qquad (17)$$

where SEE=standard error of estimate; Y=measured value (e.g., R_n measured); Y'=predicted value (e.g., R_n predicted); and n=number of observations. Net radiation (R_n) was also measured over the saltcedar and cottonwood canopy at Bosque using a Q7.1 net radiometer in 2003. The same method was used to predict daily net radiation values for both vegetations. Fig. 3 compares the predicted and measured daily net radiation values for saltcedar. The ratio of predicted over measured values in Fig. 3 was 1.02 and the SEE was 1.06 MJ/m^2/day. Fig. 4 compares the predicted and measured net radiation values for cottonwood. The ratio of predicted over measured values in Fig. 4 was 1.01 and the SEE was 1.17 MJ/m^2/day.

Method b

For the same sites, satellite data from NASA–ASTER (National Aeronautics and Space Administration–Advanced Spaceborne Thermal Emission and Reflection Radiometer) were used to calculate albedo, NDVI and surface temperature. The ASTER sensor

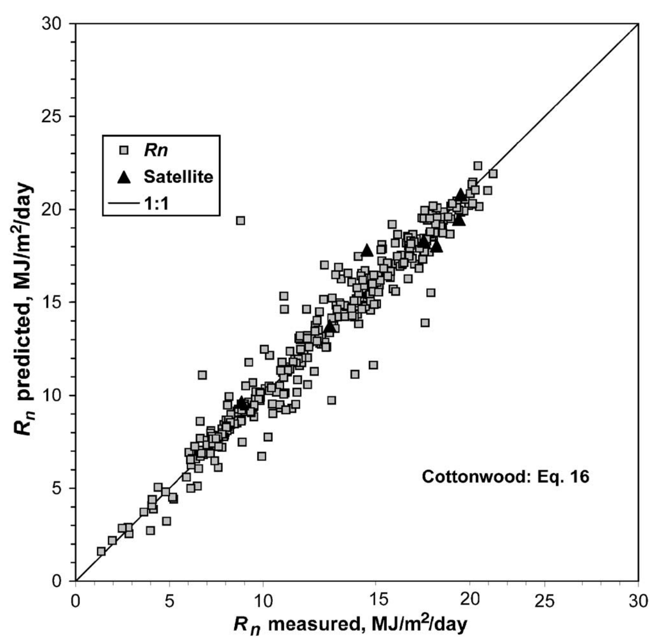

Fig. 4. Comparison between measured and estimated R_n values in cottonwood at Bosque

Table 1. ASTER Band Designations and Spectral Ranges

Subsystem	Band no.	Spectral range (μm)	Spatial resolution, m
VNIR	1	0.52–0.60	15
	2	0.63–0.69	
	3N	0.78–0.86	
	3B	0.78–0.86	
SWIR	4	1.60–1.70	30
	5	2.145–2.185	
	6	2.185–2.225	
	7	2.235–2.285	
	8	2.295–2.365	
	9	2.360–2.430	
TIR	10	8.125–8.475	90
	11	8.475–8.825	
	12	8.925–9.275	
	13	10.25–10.95	
	14	10.95–11.65	

makes multispectral observations in three wavelength regions which include visible to near infrared (VNIR), shortwave infrared (SWIR), and thermal infrared (TIR). The specific spectral ranges covered by each of the bands that the ASTER sensor uses are given in Table 1 (Abrams et al. 2002). The global coverage by ASTER is limited by several factors including the very high data rates as well as limited field of view which is 60×60 km. In addition, ASTER observations are on an "on-demand" basis and limited to about 780 scenes per day (Abrams et al. 2002) due to on-board memory and downlink bandwidth limitations.

The ASTER data used in this study came from the Land Processes Distributed Active Archive (LPDAAC—http://lpdaac.usgs.gov/main.asp) and consisted of the following:
- AST_05—surface emissivity;
- AST_07—surface reflectance (VNIR, SWIR);
- AST_08—surface kinetic temperature;
- AST_09—surface radiance (VNIR, SWIR); and
- AST_09T—surface radiance (TIR).

The data are time referenced and annotated with ancillary information, including radiometric and geometric calibration coefficients, and geolocation information. In addition the data are corrected for parameters such as atmospheric effects and variations in emissivity. The remote sensing software package ENVI, by Research Systems, Inc. (Boulder, Colo.), and its many tools were used for data processing described here. The NDVI was calculated using ASTER sensor bands 3 and 2 as

$$\mathrm{NDVI} = \frac{\rho_3 - \rho_2}{\rho_3 + \rho_2} \tag{18}$$

where ρ_i=reflectance in band i.

Different band ratios can be used to estimate the LAI (Fassnacht et al. 1997). In this study, NDVI values were used to calculate the LAI in Eq. (7). Albedo (α) was calculated using the methodology described by Liang (2001):

$$\alpha = 0.484\rho_1 + 0.335\rho_3 - 0.324\rho_5 + 0.551\rho_6 + 0.305\rho_8 - 0.367\rho_9 - 0.0015 \tag{19}$$

where ρ_i=reflectance in band i. Due to the variation related to pixel amplitude in ASTER sensor, the spatial resolutions of the calculated parameters are limited to 90 m.

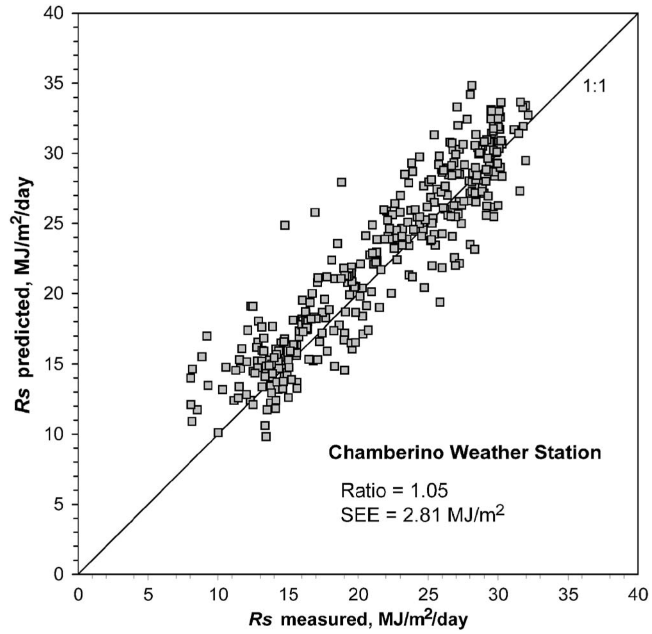

Fig. 5. Predicted and measured daily solar radiation at Chamberino Weather Station

ASTER data were available for 8 days for the pecan site and 7 days for the Bosque riparian site. Using these data, R_n values were calculated with Eqs. (1) (R_{ni}), (2) (R_{si}), and (16) (R_n). The results are shown in Figs. 2–4, as shaded triangles. The average ratios of satellite predicted over measured values were 1.05, 1.10, and 1.14 for pecan, saltcedar, and cottonwood respectively. The SEE was 1.32, 1.98, and 2.66 MJ/m^2/day for pecan, saltcedar, and cottonwood, respectively.

Method c

Method c is similar to Method b with the exception that daily solar radiation (R_s) is estimated. If measured daily solar radiations (R_s) in Eq. (16) are not available, then a methodology by Hargreaves and Samani (1982) can be used as follows:

$$R_s = K_r(T_{\max} - T_{\min})^{0.5} R_a \tag{20}$$

where $T_{\max}$ and $T_{\min}$=daily maximum and minimum air temperature (°C) and R_a=extraterrestrial radiation on daily basis and is calculated by procedures developed by Duffie and Beckman (1980, 1991) as

$$R_a = \frac{1{,}440}{\pi} G d_r[\omega_s \sin(\phi)\sin(\delta) + \cos(\phi)\cos(\delta)\sin(\omega_s)] \tag{21}$$

where G=solar constant (0.082 MJ m^2/min); d_r=inverse relative distance from earth to sun; ϕ=latitude; and ω_s=sunset hour angle (rad). d_r and δ are calculated from Eqs. (3) and (9); and ω_s is calculated from the following equation:

$$\omega_s = \arccos[-\tan(\phi)\tan(\delta)] \tag{22}$$

Allen (1995) suggested calculating K_r as

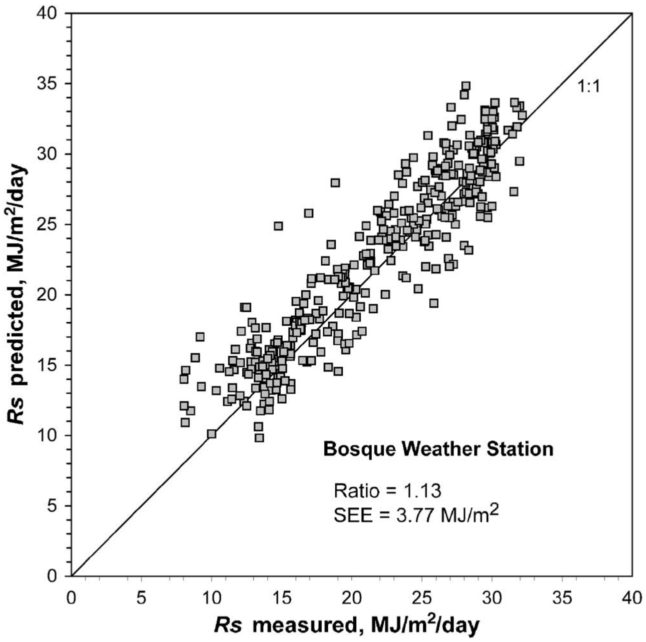

Fig. 6. Predicted and measured daily solar radiation at Bosque Weather Station

$$K_r = K_{ra}\left(\frac{P}{P_0}\right)^{0.5} \tag{23}$$

where P=mean atmospheric pressure at the site (kPa); P_0=mean atmospheric pressure at sea level (101.3 kPa); and K_{ra}=empirical coefficient equal to 0.17 for interior regions and 0.2 for coastal regions. Eq. (20) was used to estimate the daily solar radiation (R_s) values at Chamberino and Bosque Weather Stations. Figs. 5 and 6 show the comparison between measured and predicted R_s values. The average ratio of predicted over measured values in Figs. 5 and 6 were 1.05 and 1.13 and the SEE were 2.81 and 3.77 MJ/m^2/day, respectively. The weather station at Bosque was surrounded by sparsely vegetated area as opposed to the Chamberino Weather Station which was surrounded by intensively farmed area. This resulted in a higher daily temperature differential and consequently overestimated the R_s values at Bosque.

Using Method c the daily R_n values were estimated for pecan at Chamberino and riparian vegetation at Bosque. The average of predicted over net radiation were 1.11, 1.25, and 1.3 for pecan, saltcedar, and cottonwood, respectively. The SEE were 3.2, 4.89, and 5.34 MJ/m^2/day for pecan, saltcedar, and cottonwood, respectively. The results are summarized in Table 2.

The accuracy of predicted net radiation will depend on the accuracy of the pyranometer which measures the R_s. To check for the accuracy of R_s, clear sky solar radiation (R_{so}) values were calculated using a methodology recommended by Doorenbos and Pruitt (1977) and Allen et al. (1998) as

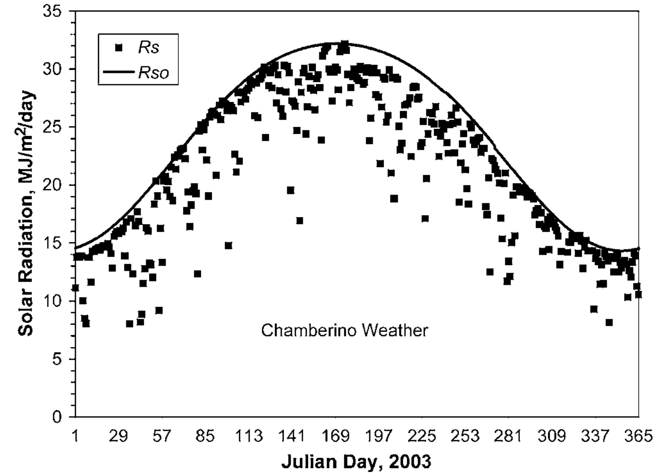

Fig. 7. Clear sky solar radiation (R_{so}) compared with measured R_s values at Chamberino Weather Station

$$R_{so} = R_a \tau_{sw} \tag{24}$$

Figs. 7 and 8 compare R_{so} values calculated from Eq. (24) with measured R_s values at Chamberino and Bosque Weather Stations. The R_{so} should plot as an upper envelope of measured R_s as a check for validity of sensor measurements. The lower measured values in Fig. 7 represent the days where R_s was less than maximum due to cloudiness.

The τ_{sw} value in Eq. (4) is described as a function of elevation (Doorenbos and Pruitt 1977; Imark et al. 2003). However the τ_{sw} value may range from 0.7 to 0.8, depending on the atmospheric clarity (dust, pollution, humidity, etc.), elevation and sun angle (Allen 1997). Majumdar et al. (1972), Boes (1981), Allen (1996), and Allen et al. (2005) have used a more complex equation to estimate τ_{sw} as

$$\tau_{sw} = K_s + K_d \tag{25}$$

where K_s=transmission coefficient for direct beam radiation (short wave radiation flux density coming directly from sun's beam) incident to a plane parallel to earth's surface and K_d=transmission coefficient for diffuse short wave radiation (short wave radiation flux density coming from scattered sunlight).

The clear sky solar radiation (R_{so}) represents the upper bound of the solar radiation values. Consistent deviation of the R_s values from R_{so} indicates a calibration problem with the pyranometer (Allen et al. 1998). The slight deviation of R_s values above the R_{so}

Table 2. Comparison of Measured and Estimated Net Radiation for Pecan, Saltcedar, and Cottonwood Using Three Methods A, B, and C

	Pecan			Saltcedar			Cottonwood		
Method	Ratio[a]	SEE[b]	n[c]	Ratio[a]	SEE[b]	n[c]	Ratio[a]	SEE[b]	n[c]
A	1.04	1.65	365	1.02	1.06	365	1.01	1.17	365
B	1.05	1.32	8	1.10	1.98	7	1.14	2.66	7
C	1.11	3.20	8	1.25	4.89	7	1.30	5.34	7

[a]Ratio=ratio of predicted over measured values.
[b]SEE=standard error of estimate.
[c]n=number of observations.

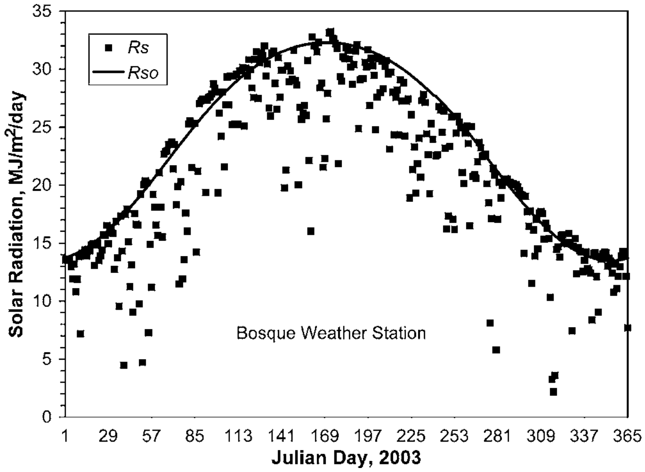

Fig. 8. Clear sky solar radiation (R_{so}) compared with measured R_s values at Bosque Weather Station

in Fig. 8, in the early spring could be due to fair weather cumulus clouds which, due to their reflectance, can drive R_s higher than that observed under a clear blue sky. The deviation can also be due to air turbidity and haziness caused by dust and aerosols (Allen et al. 2005).

Results and Conclusion

Table 2 summarizes the results of Methods a, b, and c. In Method b, the highest error of 14% occurred in cottonwood. This was due to the sparse canopy in cottonwood (about 75% cover) which resulted in a difference between point measurements of net radiation over plant surface compared with the average spatial values from satellite. Another potential source of error is the degradation of satellite based data over the pixel amplitude. In method c, the average net radiation error of 11% was observed at Chamberino Weather Station, but higher average errors of 25 and 30% occurred at Bosque Weather Station. The higher average errors at the Bosque were due to the condition of vegetation surrounding the weather station. The Chamberino Weather Station was surrounded by agriculture crops while the Bosque Weather Station was surrounded by sparse vegetation, bare soil and dry vegetation resulting in a higher daily air temperature difference and consequently an overestimation of R_s with Eq. (20).

The methodology presented here estimates the day-time net radiation which is the main driving force for evapotranspiration and other physiological activities. A procedure has been presented to estimate daily net radiation using canopy temperature, albedo, short wave radiation (R_s), and air temperature. Three methods were used to estimate day-time net radiation over plant canopy. Comparisons between measured and estimated net radiation using the three methods (a, b, and c) resulted in an average error ranging from 1 to 30% and SEE ranging from 1.06 to 5.34 $MJ/m^2/day$.

Method c resulted in the largest error compared to other methods due to error in estimating R_s. The SEE was even higher at the Bosque due to the condition of the area surrounding the weather station which resulted in larger errors in estimated R_s and consequently R_n values. Methods a and b offer the best approach in estimating day time net radiation values over vegetation. However, in the absence of daily solar radiation data, Method c could be used to estimate net radiation.

Acknowledgments

The writers acknowledge the support provided by the New Mexico Office of the State Engineer, United States Bureau of Reclamation, United States Department of Agriculture Rio Grande Basin Initiative Project, the Elephant Butte Irrigation District and United States Fish and Wildlife Service-Bosque del Apache National Wildlife Refuge.

Notation

The following symbols are used in this paper:

DT = number indicating daylight saving time;
d_r = inverse relative earth–sun distance;
ET = evapotranspiration;
G = solar constant (0.082 MJ m^2/min);
G_{sc} = solar constant (1,367 W/m^2);
J = Julian day of the year;
K_d = transmission coefficient for diffuse short wave radiation (short wave radiation flux density coming from scattered sunlight);
K_{ra} = empirical coefficient equal to 0.17;
K_s = transmission coefficient for direct beam radiation (short wave radiation flux density coming directly from sun's beam) incident to a plane parallel to earth's surface;
LAI = leaf area index;
L_{loc} = local longitude west of Greenwich (degrees);
LST = local solar time (h);
L_{std} = longitude of the standard meridian in the local time zone (degrees west of Greenwich);
n = number of observations
P = mean atmospheric pressure of the site (kPa);
P_0 = mean atmospheric pressure at sea level (101.3 kPa);
R_a = extraterrestrial radiation on daily basis ($MJ/m^2/day$);
R_n = net radiation (W/m^2);
R_{ni} = incident (instantaneous) net radiation (W/m^2);
R_s = short wave radiation (W/m^2);
R_{si} = incident incoming short wave radiation (W/m^2);
R_{so} = clear sky solar radiation ($MJ/m^2/day$);
$RL\downarrow$ = incident incoming longwave radiation (W/m^2);
$RL\uparrow$ = incident outgoing longwave radiation (W/m^2);
S_c = correction (h), which accounts for perturbation in earth's rotation rate;
SEE = standard error of estimate;
T_a = average daily air temperature (K);
T_i = incident near surface air temperature (K);
T_{max} = daily maximum air temperature (°C);
T_{min} = daily minimum air temperature (°C);
T_s = incident surface temperature (K);
t = local civil time (Pacific Standard Time, Eastern Standard Time, etc.);
Y = measured value;
Y' = predicted value;
Z = elevation (m);
α = surface albedo (dimensionless);
β = downward slope, where $\beta=0$ for horizontal surface and $\beta=\pi/2$ for vertical;
γ = deviation of the normal to the surface from the local meridian;
δ = solar declination (rad);
ε_a = atmospheric emissivity;

ε_0 = surface emissivity (dimensionless);
θ = solar incidence angle;
ρ_i = reflectance in band i.
σ = Stefan–Boltzman constant (5.67×10^{-8} W/m^2/K^4);
τ_{sw} = atmospheric transmissivity from elevation surface;
ϕ = latitude of the site;
ω = solar time angle (rad); and
ω_s = sunset hour angle (rad).

References

Abrams, M., Hook, S., and Ramachandran, B. (2002). *ASTER user's handbook, version 2*, Jet Propulsion Laboratory, Pasadena, Calif.

Allen, R. G. (1995). "Evaluation of procedures for estimating mean monthly solar radiation from air temperature." *Rep.*, Food and Agricultural Organization of the United Nations (FAO), Rome.

Allen, R. G. (1996). "Assessing integrity of weather data for reference evapotranspiration estimation." *J. Irrig. Drain. Eng.*, 122(2), 97–106.

Allen, R. G. (1997). "Self-calibrating method for estimating solar radiation from air temperature." *J. Hydrol. Eng.*, 2(2), 56–97.

Allen, R. G., Pereira, L. S., Raes, D., and Smith, M. (1998). "Crop evapotranspiration. Guidelines for computing crop water requirements." *FAO Irrigation and Drainage Paper No. 56*, Food and Agricultural Organization of the United Nations, Rome.

Allen, R. G., Walter, I. A., Elliott, R. L., Howell, T. A., Itenfisu, D., Jensen, M. E., and Snyder, R. L., eds. (2005). *The ASCE standardized reference evapotranspiration equation*, American Society of Civil Engineers, Reston, Va.

Bastiaanssen, W. G. M. (1995). "Regionalization of surface flux densities and moisture indicators in composite terrain: A remote sensing approach under clear skies in Mediterranean climates." Ph.D. dissertation, Landbouwuniversiteit te Wageningen, Wageningen, The Netherlands.

Boes, E. C. (1981). "Fundamentals of solar radiation." *Solar energy handbook*, J. F. Kreider and F. Kreith, eds., McGraw-Hill, New York, Chap. 2.

Doorenbos, J., and Pruitt, W. O. (1977). "Guidelines for prediction of crop water requirements." *FAO Irrigation and Drainage Paper No. 24 (revised)*, Food and Agricultural Organization of the United Nations, Rome.

Duffie, J. A., and Beckman, W. A. (1980). *Solar engineering of thermal processes*, 1st Ed., Wiley, New York.

Duffie, J. A., and Beckman, W. A. (1991). *Solar engineering of thermal processes*, 2nd Ed., Wiley, New York.

Fassnacht, K. S., Gower, S. T., MacKenzie, M. D., Nordheim, E. V., and Lillesand, T. M. (1997). "Estimating the leaf area of north central Wisconsin forests using the Landsat Thematic Mapper." *Remote Sens. Environ.*, 61, 229–245.

Hargreaves, G. H., and Samani, Z. A. (1982). "Estimating potential evapotranspiration." *J. Irrig. Drain. Eng.*, 108(3), 225–230.

Irmak, S., Irmak, A., Jones, J. W., Howell, A., Jacobs, A. M., Allen, R. G., and Hoogenboom, G. (2003). "Predicting daily net radiation using minimum climatological data." *J. Irrig. Drain. Eng.*, 129(4), 256–269.

Liang, S. (2001). "Narrowband to broadband conversion of land surface albedo. I. Algorithms." *Remote Sens. Environ.*, 76, 213–238.

Majumdar, N. C., Mathur, B. L., and Kaushik, S. B. (1972). "Prediction of direct solar radiation for low atmospheric turbidity." *Sol. Energy*, 13, 383–394.

Recktenwald, G. (2004). "Solar radiation and solar angles." Mechanical Engineering Dept., Portland State Univ., Portland, Ore.

Rosenberg, N. J., Blad, B. L., and Verma, S. B. (1983). *Microclimate—The biological environment*, Wiley, New York.

Samani, Z., Nolin, S., Bleiweiss, M., and Skaggs, R. (2005). "Discussion of Predicting Daily Net Radiation Using Minimum Climatological Data." *J. Irrig. Drain. Eng.*, 131(4), 388–389.

Tasumi, M., Allen, R., and Kramber, W. (2000). *Application of the SEBAL methodology for estimating consumptive use of water and stream flow depletion in the Bear River Basin of Idaho through remote sensing*. Idaho Department of Water Resources and the University of Idaho, Department of Biological and Agricultural Engineering, Moscow, Id.